Int. J. Heat Mass Transfer. Vol. 36, No. 7, pp. 1807–1818, 1993
Printed in Great Britain

0017-9310/93 $6.00 + 0.00
Pergamon Press Ltd

# Determination of transfer coefficients by psychrometry

A. KONDJOYAN and J. D. DAUDIN
Institut National de la Recherche Agronomique, Station de Recherche sur la Viande, Theix 63122 St-Genes-Champanelle, France

(*Received* 14 *December* 1990 *and in final form* 25 *May* 1992)

**Abstract**—This paper presents a method based on psychrometry for measuring simultaneously heat and mass transfer coefficients in the case of forced convective exchanges between air and a body surface. This method is specially well adapted to bodies of complex shapes. The theoretical aspects are described. Errors linked to data treatments and to measurements are discussed. The method is tested for a circular cylinder in cross flow in the following conditions: $3500 < Re < 26\,000$, $Tu = 12\%$, $T_{air} = 25°C$. Discussion shows that errors can be reduced to less than 2% for mean transfer coefficients and less than 5% for local coefficients.

## 1. INTRODUCTION

HEAT OR MASS transfers between air and products are involved in many food industry processes. To control these events it is necessary to know the mean transfer coefficients which determine the mean flux exchanges and hence the treatment lengths and apparatus functioning. It is also important to know the local values of these coefficients around the treated bodies as the transfer intensity affects temperature changes and water concentrations and consequently the local rates of enzymatic and microbial reactions. The heterogeneity of microbial growth and of colour and flavour changes has a direct influence on food product quality.

For studying these air–product exchanges in conditions close to the food industries, the coefficients should be known in the following situations: (1) low air velocity (0.1 to 5 m $s^{-1}$), (2) turbulent flow, (3) bodies of complex, irregular and various shapes, (4) small temperature differences at the body surface.

The classical method for measuring heat transfer coefficients is constraining and limited. It assumes that the shape is fully surrounded by an electrical ribbon providing a constant heat flux. Great differences are observed between the surface temperatures. Hence the temperature has to be measured at many points. The heat transfer coefficients determined with this method are different from those existing during most of the food processes in which the temperature at the body surface is nearly uniform.

Mass transfer coefficients are usually determined from other experiments based on the adiabatic evaporation of liquid or sublimation of solid (naphthalene).

These experiments used to determine heat or mass transfer coefficients cannot be performed when the body shape is complex.

To cope with these failures, we developed a method for measuring the heat and mass transfer coefficients on the basis of the 'psychrometric exchanges'. Psychrometry is universally used to determine air relative humidity. An experimental procedure based on this phenomenon has the advantage of supplying a simultaneous measure of heat and mass transfer coefficients around a body whose shape and form can be complex. The distributions of the temperatures on the object are similar to those existing at the surface of the product during a food process. Besides, the preparation of the bodies is simple and rapid.

## 2. THEORETICAL APPROACH

*Transfers by air convection*

In the air, provided that there is no influence of mass transfers on heat transfers and vice versa, the transfer equations are as follows (D/D$t$ represents the substantive derivative):

$$\rho c_p \frac{D(T)}{DT} = \lambda \nabla^2(T) \tag{1}$$

$$\frac{D(C)}{Dt} = D\nabla^2(C). \tag{2}$$

In the case of an exchange between a body surface and air, (1) and (2) become in contact with the wall:

$$\phi_t = \lambda(\partial T/\partial y)_{y=0} \tag{3}$$

$$\phi_m = D(\partial C/\partial y)_{y=0} \tag{4}$$

$\phi_t$ and $\phi_m$ being the heat and mass fluxes exchange at the interface air-product. In thermic and chemical engineering, (3) and (4) are classically simplified to:

$$\phi_t = h(T_\infty - T_w) \tag{5}$$

$$\phi_m = k'(C_\infty - C_w). \tag{6}$$

When introducing the dimensionless coordinates, $\theta$ and $G$, we get immediately from (3)–(6):

## NOMENCLATURE

| | |
|---|---|
| $C$ | water vapor concentration in air [kg m$^{-3}$] |
| $c_p$ | specific heat of air [J kg$^{-1}$ K$^{-1}$] |
| $D$ | water diffusivity in air [m$^2$ s$^{-1}$] |
| $d$ | cylinder diameter [m] |
| $E$ | general symbol for relative error |
| $G$ | dimensionless concentration of water, $(C-C_w)/(C_\infty-C_w)$ |
| $h$ | heat transfer coefficient [W m$^2$ K$^{-1}$] |
| $j_H$ | Chilton–Colburn $j$ factor for heat transfer, $Nu\,Re^{-1}\,Pr^{-1/3}$ |
| $j_D$ | Chilton–Colburn $j$ factor for mass transfer, $Sh\,Re^{-1}\,Sc^{-1/3}$ |
| K | constant defined in equation (26) |
| $k'$ | mass transfer coefficient defined in equation (8) [m s$^{-1}$] |
| $k$ | mass transfer coefficient [kg m$^{-2}$ (Pa s)$^{-1}$] |
| $L$ | body perimeter [m] |
| $l$ | streamwise coordinate along surface from front stagnation point [m] |
| *Lewis* | Lewis number |
| $L_{vap}$ | latent heat of evaporation of water [J kg$^{-1}$] |
| $M_{air}$ | 'molecular' weight of air [kg] |
| $M_{water}$ | 'molecular' weight of water [kg] |
| $Nu$ | Nusselt number, $hd/\lambda$ |
| $P$ | general symbol for pressure [Pa] |
| $P_{atm}$ | atmospheric pressure [Pa] |
| $P(T)$ | saturated water vapour pressure at temperature $T$ [Pa] |
| $Pr$ | Prandtl number |
| $S$ | body surface [m$^2$] |
| $Sc$ | Schmidt number |
| $Sh$ | Sherwood number, $k'd/D$ |
| $T$ | air temperature [°C or K] |
| $T_{dew}$ | dew point temperature [°C or K] |
| $T_H$ | wet bulb temperature [°C or K] |
| $Tu$ | turbulence intensity of air in the main stream direction, $\sqrt{\bar{u}^2}/U_\infty$ |
| Vel | general symbol for air velocity [m s$^{-1}$] |
| $u$ | velocity fluctuation around $U$ [m s$^{-1}$] |
| $U$ | velocity in the main stream direction outside the boundary layer [m s$^{-1}$] |
| $y$ | coordinate normal to surface [m]. |

Greek symbols

| | |
|---|---|
| $\alpha$ | angular coordinate from front stagnation point [rad or degrees] |
| $\varepsilon$ | plaster emissivity |
| $\Phi_{rad}$ | heat flux exchanged by radiation [W m$^{-2}$] |
| $\Phi_t$ | heat flux exchanged by convection between body surface and air [W m$^{-2}$] |
| $\Phi_m$ | mass flux exchanged between body surface and air [kg m$^{-2}$ s$^{-1}$] |
| $\Phi_{ech}$ | energy balance between body and air [W m$^{-2}$] |
| $\theta$ | dimensionless temperature $(T-T_w)/(T_\infty-T_w)$ |
| $\lambda$ | thermal conductivity [W m$^{-1}$ K$^{-1}$] |
| $\rho_{air}$ | density of air [kg m$^{-3}$] |
| $\sigma$ | Stefan–Boltzmann constant [W m$^{-2}$ K$^{-4}$] |
| $\mu$ | dynamic viscosity [kg m$^{-1}$ s$^{-1}$] |
| $\nu$ | kinematic viscosity [m$^2$ s$^{-1}$]. |

Subscripts

| | |
|---|---|
| w | wall condition |
| $\infty$ | free stream condition. |

Mean

| | |
|---|---|
| $\bar{x}$ | mean of $x$. |

$$h = \lambda(\partial\theta/\partial y)_{y=0} \tag{7}$$

$$k' = D(\partial G/\partial y)_{y=0}. \tag{8}$$

It follows that:

$$\frac{h}{k'} = \rho c_p Lewis \frac{(\partial\theta/\partial y)_{y=0}}{(\partial G/\partial y)_{y=0}} \tag{9}$$

with:

$$Lewis = \frac{(\lambda/\rho c_p)}{D} = \frac{Sc}{Pr}. \tag{10}$$

In fact it has been shown theoretically for local coefficients in the case of a laminar flow over a flat plate, Ozisik [1], and confirmed experimentally for a turbulent flow on a liquid surface, Katto *et al.* [2] that with $n = 2/3$:

$$\frac{h}{k'} = \rho c_p (Lewis)^n. \tag{11}$$

This relation can be inferred from Chilton–Colburn's analogy which was first evidenced in tubes and on flat plates. Actually the equality of the factors $j_H$ and $j_D$, leads to the conclusion:

$$\frac{j_H}{j_D} = \frac{h}{k'}\frac{1}{\rho c_p}(Lewis)^{-2/3} = 1. \tag{12}$$

In this study only the ratio of $j_H$ to $j_D$ is important because only the relation of heat to mass transfer is of interest and not other relations which involved momentum.

For circular cylinders in a cross flow, Kestin and Wood [3] used the relation (11) with $n = 2/3$ to deter-

mine the wall temperatures and so the local mass transfer coefficient before and after the separation of the boundary layer. Lewis [4] calculated $h/(\rho c_p k')$ in the form of the ratio of the heat to the mass Stanton numbers for two cases: for the laminar boundary layer corrected with the wedge flow theory and for the front laminar and rear separated region of the cylinder according to Richardson's theory. In both cases $h/(\rho c_p k')$ values differ by less than 7.5% from $(Lewis)^{2/3}$. Dahlen [5] studied the relation between the mean heat and mass transfer coefficients for adiabatic evaporation of several fluids (benzene, acetone, carbon tetrachloride, water) from the cylinder surface. The experimental results showed that in each case the Chilton–Colburn factor of mass transfer, $j_D$, was equal to the Chilton–Colburn factor of heat transfer, $j_H$. Moreover for water and only for water, for a given Reynolds number, the value of $j_H$ and $j_D$ was surprisingly constant whatever the evaporation rate at the cylinder surface. Martin and Lebouché [6] show that when Schmidt and Prandtl numbers are very different ($Sc > 1000$ and $Pr < 10$) the Chilton–Colburn analogy must be corrected depending on the Reynolds number. This analogy can even be false in the wake of the circular cylinder. But these authors noted that when the values of the Schmidt and Prandtl numbers are similar (for example for air $Pr = 0.73$ at $T = 20°C$ and naphthalene $Sc = 2.44$) Chilton–Colburn's analogy fits well.

For a sphere placed in a flow at various turbulence intensities, Torii *et al.* [7], on the basis of mean heat and mass transfer measurements verified the relation (11) but with the $n$ exponent ranging between 0.4 and 0.5.

The values suggested by the different authors are given in Table 1. The experimental result tends to prove that over a flat plate, a cylinder, a sphere, the $(\partial\theta/\partial y)_{y=0}/(\partial G/\partial y)_{y=0}$ ratio is constant at any point of the body surface and equal to $(Lewis)^p$ with $p = n-1$.

These studies tend to prove that whatever the form of a fully wetted body (flat plate, circular cylinder, sphere), placed in a laminar or turbulent cross air stream, when the values of Schmidt and Prandtl numbers are close (for water evaporation in air $Sc = 0.63$ and $Pr = 0.73$ at $T = 20°C$) relation (11) is confirmed with $n$ ranging from 0.4 to 0.66. Whatever the value of $n$, $h/k'$ is constant at any point of the body surface (before and after the separation) and is equal to the ratio between the mean transfer coefficients.

In studies related to drying the water flux from the product to the air $\phi_m$ (6) is usually written in the form:

$$\phi_m = k(P(T_{dew}) - P_w). \tag{13}$$

$P_w$ and $P(T_{dew})$ are the water vapour pressures at the body surface and in air and:

$$k = k' \frac{M_{water}\rho_{air}}{M_{air}P_{atm}}. \tag{14}$$

It then follows, according to (11):

$$\frac{h}{k} = c_p \frac{M_{air}P_{atm}}{M_{water}} (Lewis)^n. \tag{15}$$

*Drying and psychrometry*

Since the early work of Sherwood [8] it has been shown by many workers and summarised in engineering books (Brennan *et al.* [9], Geankoplis [10], Bimbenet [11] and Loncin and Merson [12]) that the drying of a solid with air of constant properties consists of three successive main stages: (1) a 'settling down' period during which the solid surface conditions come into equilibrium with the drying air, (2) a 'steady-state' or 'constant rate' period and

Table 1. Literature data relative to the heat and mass transfer analogy ($n$ is the exponent of the Lewis number)

| Work type | Incident air flow | Reynolds range | Type of mass transfer | Shape | $n$ | Reference |
|---|---|---|---|---|---|---|
| exp | ? | ? | water vapour | ? | 1 | Lewis (1922) |
| exp+theo | laminar | ? | water vapour | flat plate | 2/3 | Coburn and Chilton (1933) |
| exp+theo | laminar | $800 < Re < 1000$ | water vapour acetone benzene | circular cylinder | 2/3 | Dahlen (1962) |
| exp | $Tu > 0.2\%$ $Tu < 7.3\%$ | $75 < Re < 125\,000$ | paradichloro-benzene | circular cylinder | 2/3 | Kestin (1971) |
| exp | laminar | $5\times10^3 < Re < 120\,000$ | naphthalene | circular cylinder | 2/3 | Lewis (1971) |
| exp | turbulent | $7\times10^3 < Re < 140\,000$ | water vapour | liquid surface | 2/3 | Katto (1975) |
| exp | $Tu > 0.3\%$ $Tu < 8.5\%$ | $3\times10^3 < Re < 140\,000$ | naphthalene | sphere | 0.4–0.5 | Torii (1981) |
| theo | laminar or turbulent | | $Pr > 1$, $Sc > 1$ $Pr$, $Sc$ near 0 | flat plate flat plate | 2/3 0.5 | Ozisik (1985) |

(3) a 'falling rate' period which begins when the surface is no more fully wetted, that is when the water vapour pressure at any point of the solid surface starts to fall under the saturated vapour pressure.

During the steady-state period exchanges by adiabatic compression and friction are usually minor since the Mach number is low [13]. Fluxes exchanged between the air and the surface of a wetted body are, $\phi_t$ convective and $\phi_{rad}$ radiative heat fluxes, as well as an energy flux depending on the evaporation, $\phi_m L_{vap}$. If the whole environment of the body is at air temperature and considered as a black body, the ratio of the body surface to the environment surface very small, and the body emissivity considered as constant with time:

$$\phi_{rad} = \varepsilon\sigma(T_\infty^4 - T_w^4). \quad (16)$$

As long as the surface is fully wetted $P_w = P(T_w)$ and the energy balance between the air and the body is:

$$\phi_{ech} = kL_{vap}(P(T_{dew}) - P(T_w)) + h(T_\infty - T_w) + \varepsilon\sigma(T_\infty^4 - T_w^4). \quad (17)$$

The steady-state period is generally well marked for capillary-porous non-hygroscopic materials like sand, chalk, plaster etc. It is characterised by a constant rate of the mass transfer $\phi_m$ and by the constancy of the temperatures at any point of the solid surface. At the same time the water concentration profiles inside the solid vary greatly, as shown by Maneval *et al.* [14] from NMR images, particularly at the surface, but the rate of water transfer from inside the solid to the surface is high enough to maintain any point of the surface fully wetted, i.e. the water vapour pressure is equal to the saturated vapour pressure $P(T_w)$. During the steady-state period the energy supplied to the surface exactly compensates the energy removed by evaporation, thus $\phi_{ech} = 0$ in equation (17). If in addition the amount of heat exchanged by radiation is negligible relative to that exchanged by convection, the surface temperature at any surface point of the body is equal to the so-called wet bulb temperature which depends only upon the air temperature and humidity. In practice this property is used to derive air humidity from the temperature given by a thermometer covered by a wetted wick and placed in an air stream. To render the exchange by radiation unimportant the air velocity must be higher than 1 m s$^{-1}$ [11, 12].

*Determination of mean transfer coefficients during the steady-state period*

By integration of (13) over the whole body surface:

$$\int_s \phi_m \, ds = \int_s k(P(T_{dew}) - P(T_w)) \, ds \quad (18)$$

using the average values, $\bar{\phi}_m$, $\bar{T}_w$, $\bar{h}$, $\bar{k}$ it follows:

$$S\bar{\phi}_m = \int_s k(P(T_{dew}) - P(\bar{T}_w)) \, ds - \int_s k(P(T_w) - P(\bar{T}_w)) \, ds \quad (19)$$

leading to an expression for $\bar{k}$:

$$\bar{k} = \frac{\bar{\phi}_m}{(P(T_{dew}) - P(\bar{T}_w))} + \frac{\int_s k(P(T_w) - P(\bar{T}_w)) \, ds}{S(P(T_{dew}) - P(\bar{T}_w))}. \quad (20)$$

Using (17) the same development leads to:

$$\bar{h} = \frac{-\bar{\phi}_m L_{vap}}{(T_\infty - \bar{T}_w)} - \frac{\varepsilon\sigma(T_\infty^4 - (\bar{T}_w)^4)}{(T_\infty - \bar{T}_w)} + \frac{\int_s (h(T_w - \bar{T}_w) + \varepsilon\sigma(T_w^4 - (\bar{T}_w)^4)) \, ds}{S(T_\infty - \bar{T}_w)}. \quad (21)$$

With low air velocities ($U_\infty < 2.0$ m s$^{-1}$) and large bodies, the radiation is low, but not nonexistent. The surface temperatures, $T_w$, exceed the wet bulb temperature of the air $T_H$, and are different from one body point to another. The mean transfer coefficients can then be determined during the steady-state period by equations (22) and (23):

$$\bar{h} = \frac{-\bar{\phi}_m L_{vap}}{(T_\infty - \bar{T}_w)} - \frac{\varepsilon\sigma(T_\infty^4 - (\bar{T}_w)^4)}{(T_\infty - \bar{T}_w)} \quad (22)$$

$$\bar{k} = \frac{\bar{\phi}_m}{(P(T_{dew}) - P(\bar{T}_w))} \quad (23)$$

with relative errors of $E_{1h}$ and $E_{1k}$, respectively, on $\bar{h}$ and $\bar{k}$, due to the method:

$$E_{1h} = \frac{1}{\bar{h}S(T_\infty - \bar{T}_w)} \int_s (h(T_w - \bar{T}_w) + \varepsilon\sigma(T_w^4 - (\bar{T}_w)^4)) \, ds \quad (24)$$

$$E_{1k} = \frac{1}{\bar{k}S(P(T_{dew}) - P(\bar{T}_w))} \int_s k(P(T_w) - P(\bar{T}_w)) \, ds. \quad (25)$$

If higher air velocities at any point of the surface radiation is negligible then $E_{1h} = E_{1k} = 0$. In the case of a cylinder of infinite length placed in a bi-dimensional cross-flow, the surface $S$ in equations (24) and (25) can be replaced by the circumferential length of the body, $L$, and $ds$ by $dl$, $l$ representing the surface length from the stagnation point.

In addition to the errors depending on the calculation method, $E_{1h}$ and $E_{1k}$, the relative errors, $E_{2h}$ and $E_{2k}$, depending on the measurement, should be evaluated. The errors can be easily obtained by differentiation of (22) and (23). Two cases must be distinguished: (1) the measurement errors on the mean mass flux $\Delta(\phi_m)$, on the air temperature $\Delta(T_\infty)$

and on the surface temperatures $\Delta(T_w)$ are independent; (2) the air and surface temperatures are measured with the same probe (error $\Delta(T)$). In both cases $(T_\infty - T_w)$ and $(P(T_w) - P(T_{dew}))$, which tend to minimise $E_{2h}$ and $E_{2k}$, should be increased, which means a rise of the air temperature. The consecutive increase in $dP(T_w)/dT_w$ and hence in $E_{2k}$ suggests that there is an optimum temperature for the determination of $\bar{k}$.

*Determination of local transfer coefficients during the steady-state period*

As discussed before, assuming that $h/k$ is constant, $K$ is defined by:

$$K = \frac{h}{kL_{vap}} = \frac{\bar{h}}{\bar{k}L_{vap}}. \quad (26)$$

During the steady-state period, it follows from (17):

$$h = \frac{\varepsilon\sigma(T_\infty^4 - T_w^4)}{(T_w - T_\infty) + (P(T_w) - P(T_{dew}))/K} \quad (27)$$

$$k = \frac{\varepsilon\sigma(T_\infty^4 - T_w^4)}{L_{vap}[K(T_w - T_\infty) + (P(T_w) - P(T_{dew}))]}. \quad (28)$$

Equations (27) and (28) are true at any point of a flat or convex surface since in that case the solid angle between the body surface and the experimental chamber walls, whose temperature is $T_\infty$, is $\Pi$. In the case of points of a concave surface, the expression $\varepsilon\sigma(T_\infty^4 - T_w^4)$ should be corrected by a factor taking into account the reduction of the solid angle.

There are two routes for calculating $h$ and $k$; constant $K$ can be a theoretical value, $K_{th}$, determined by equation (15), or an experimental value, $K_{exp}$, calculated from mean values $\bar{h}$ and $\bar{k}$ obtained during the same trial. The relative errors on $h$ and $k$ are identical since the ratio $h/k$ is constant. When differentiating equation (27), we get:

$$dh/h = H1\, dT_\infty + H2\, dT_w + H3\, dT_{dew} \quad (29)$$

with $H1$, $H2$, $H3$ functions of $T_\infty$, $T_{dew}$, $T_w$, $K_{th}$, $K_{exp}$.

When $H1$, $H2$, $H3$ are calculated by means of constant $K_{th}$ or $K_{exp}$, assuming that $\Delta(T_\infty) = \Delta(T_w) = \Delta T_{dew} = \Delta T$ and that all temperature measurements are independent of each other, the relative error on the transfer coefficients is:

$$\Delta h/h \leqslant (|H1| + |H2| + |H3|)\Delta T. \quad (30)$$

If the two temperatures, $T_\infty$ and $T_w$, are measured with the same probe temperature

$$\Delta h/h \leqslant (|H1 + H2| + |H3|)\Delta T. \quad (31)$$

## 3. EXPERIMENTAL PROCEDURE

The purpose of these experiments was to test the psychrometric method used to determine mean and local heat and mass transfer coefficients around a circular cylinder, which is the most studied body in the literature.

*Apparatus*

The experiments were carried out in a closed circuit controlled-environment chamber, designed for studies on chilling of foodstuffs, which has been described in detail in a previous paper, Daudin and Swain [15]. The chamber is composed of two vertical working cells (0.5 $m^2$ in section, 1 m in height) (Fig. 1). The air temperature and dew point temperature in the chamber can be kept constant and measured with an accuracy of $\pm 0.1°C$. The average air velocity was controlled with an accuracy of 0.05 m $s^{-1}$.

In a preliminary trial, the air velocity was measured at 44 locations in each cell. The results are reported in Table 2, the range of variation was 10% from one place to another. The values quoted are the average air velocities corresponding to the empty chamber. The free stream turbulence intensity ($Tu$) was measured where the samples were located during the experiments, with a constant temperature hot wire anemometer equipped with a linearising circuit. Results are given in Table 3. The turbulence intensity was always close to 12% and a little higher in cell 2 than in cell 1. The turbulence intensity tended also to increase as the air velocity decreased.

*Samples*

It was decided to use plaster to make the cylinders for three reasons:

(i) it is a rigid permeable material which hydrates easily,

(ii) it has been shown to remain fully wetted during most of a drying process, Fornell [16], Kondjoyan [17],

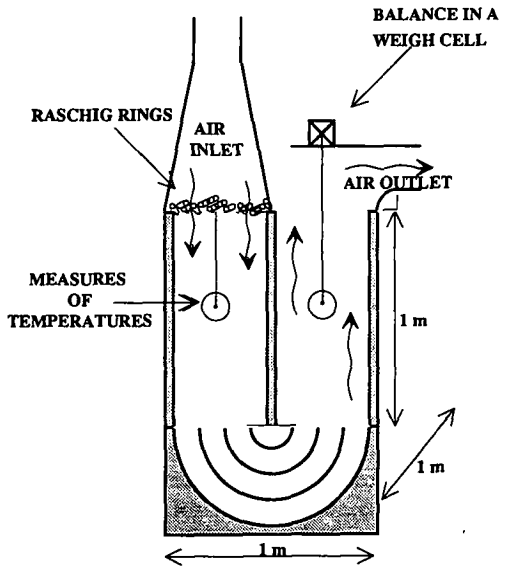


FIG. 1. Schematic representation of the experimental chamber.

Table 2. Average and standard deviation of air velocity in the experimental cells

| Experiment number | Average air velocity (m s$^{-1}$) | | Standard deviation (m s$^{-1}$) | |
|---|---|---|---|---|
| | First cell | Second cell | First cell | Second cell |
| 1 | 2.15 | 2.20 | 0.26 | 0.27 |
| 2 | 1.18 | 1.20 | 0.13 | 0.14 |
| 3 | 0.49 | 0.51 | 0.04 | 0.06 |

Table 3. Measured turbulence intensity in the experimental cells for different air velocities

| Average air velocity (m s$^{-1}$) | First cell | Second cell |
|---|---|---|
| 0.5 | 13 | 17 |
| 1.0 | 11 | 14 |
| 1.5 | 10 | 11 |
| 2.0 | 10 | 10 |

(iii) it will be readily used in the future to make bodies of complex shape.

Two samples, like those in Fig. 2, were used in each experiment. At points 1–5, in one of the samples, five thermocouples were inserted to measure the temperature ($\pm 0.1$°C) 1 mm below the surface. The other sample was used for weight loss measurement ($\pm 0.1$ g). The portion of the plaster sample subjected to air exchanges was inserted between plastic discs, to prevent both water transfer and heat conduction perpendicular to the main flow. Wooden discs were added to eliminate edge fringing in the measurements areas. These discs were varnished and covered with a plastic film to prevent any evaporation from the wood surface.

*Experimental conditions*

Each experiment was carried out with constant air properties: temperature, humidity and velocity. The air temperature was 25°C and the relative humidity was about 20%. This low humidity was chosen in order to obtain large mass and heat transfer driving forces, $(P(T_{dew}) - P(T_w))$ and $(T_\infty - T_w)$. Four average air velocities (0.5, 1.0, 1.5, 2.0 m s$^{-1}$) and three cylinder diameters (0.10, 0.15, 0.20 m) were considered.

The plaster cylinders were soaked with the thermocouples in place at least 10 h in a water bath for hydration. The bath temperature was set at the assumed air wet bulb temperature of the experiment in order to shorten as much as possible the 'settling-down' period. After the plaster cylinders were removed from the bath, the excess of water was

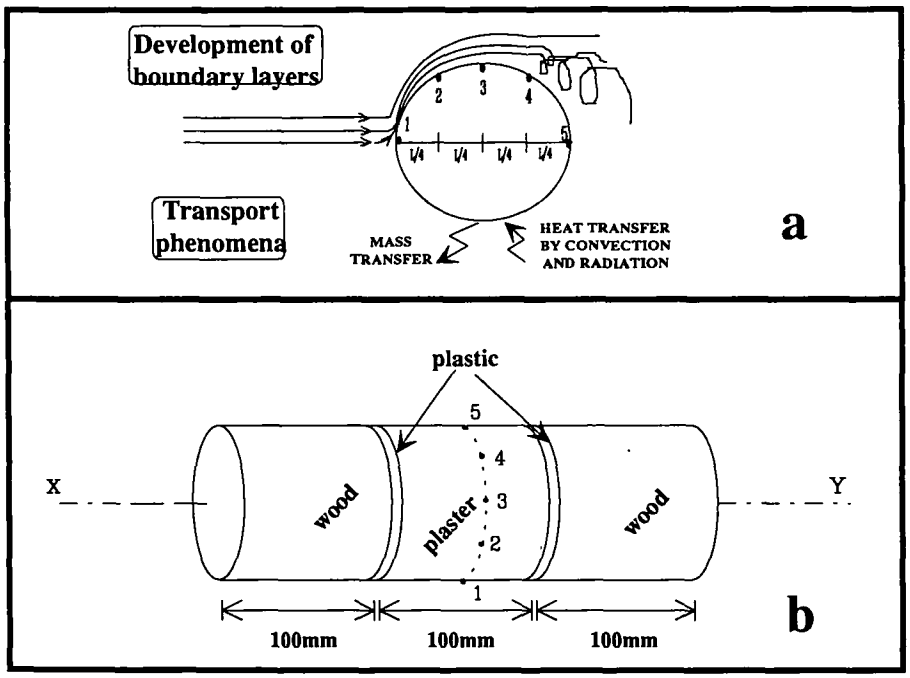


FIG. 2. (a) Schematic representation of air flow over a sample and of transport phenomena; (b) diagrams of the samples.

drained, wiped off and the samples were assembled as in Fig. 2. One sample was put in the first cell to measure the temperatures, the other was suspended from the balance situated above the second cell. The air properties and sample temperatures were recorded every 2 min by a Hewlett-Packard data logging system. The balance was connected to a computer and the sample weight was averaged every 2 min from 100 measurements performed in less than 2 s.

All experiments were performed twice.

*Calculations*

Calculations were performed during the steady-state period using $\varepsilon = 0.91$, Mohsenin [18]. According to the balance accuracy $\pm 0.1$ g, $\bar{\phi}_m$ was calculated by linear regression from weight loss measurements with a relative error lower than $10^{-3}$. Thus the error on $\bar{\phi}_m$ was always omitted. The variation of $T_w$ was assessed over the whole body surface by a polynomial regression based on the five temperature measurements. $\bar{T}_w$ was then calculated by an integration procedure with an accuracy of about 0.1°C. The amount of heat exchanged by radiation was determined by equation (16). Mean coefficients $\bar{h}$ and $\bar{k}$ were then determined by equations (22) and (23), the method errors by equations (24) and (25). Local coefficients $h$ and $k$ were calculated at the temperature measurement points by equations (27) and (28). The measurement errors were determined by equations coming from the differentiation of (22) and (23) and (27) for the different cases discussed above.

## 4. RESULTS AND DISCUSSION

*Body surface temperatures*

The typical results of an experiment are given in Fig. 3(a). After a settling-down period of about 3 h the surface temperatures reached their 'equilibrium' value and then remained constant for several hours. At the same time the water flux increased slowly and reached a constant value as indicated by the slope of the weight loss curve. This confirms the existence of a steady-state simultaneous heat and mass transfer. A few hours later the temperature at the stagnation point, where exchanges were the most intensive, rose swiftly and was close to air temperature in approximately 1 h.

During all the experiments the surface temperatures were higher than the wet bulb temperatures. Figure 3(b) shows the difference between surface temperatures and wet bulb temperature on the circular cylinder, 0.1 m in diameter for the four air velocities. The lower the air velocity, the higher the surface temperatures. For the same air velocity, the surface temperature, minimum at the stagnation point, increased up to a maximum, close to the separation point, and then decreased. The difference was rather small between the various surface temperatures per trial: 1.0°C on an average throughout the experiment.

The wet bulb temperature was calculated from the measured dew point temperature by taking into account corrections depending on the laboratory altitude ($P_{atm} = 91\,990$ Pa) and by considering $T_H$ equal to the air adiabatic saturation temperature. This identity is widely accepted in the literature and corresponds to $n = 2/3$ in (11). If $n$ were not 2/3 but 0.4, the minimum value which is given by the literature, the calculated $T_H$ would be at most 0.2°C higher. So according to theory of drying, the $T_w - T_H$ differences must be attributed to a radiative heat transfer from the surrounding to the sample surface. These differences are perfectly in keeping with the theory relative to the development of boundary layers: the smaller the $h$ value, due to either a low air velocity or to the thickening of the thermal boundary layer, the more marked the effect of radiation, increasing the $T_w - T_H$ difference.

It should be noticed that the exact value of $T_H$ is not of great interest because $T_H$ is not involved in the calculation of $h$ and $k$.

*Mean transfer coefficients*

The results obtained with the psychrometric method in the form of $Nu = f(Re)$ and those derived from Hilpert (turbulence intensity close to 0%) as well as those from Dyban *et al.* [19] (two turbulence intensities of 0.3, 12%) are compared in Fig. 4. Hilpert's values are considered by several authors, MacAdams [20], Morgan [21], and more recently Ota [22] as reference values for a circular cylinder placed in a cross flow with no turbulence. These values were, however, systematically 30% lower than those measured by Dyban for $Tu = 0.3\%$ in the considered field of Reynolds.

The values determined by the psychrometric method, with a turbulence intensity close to 12%, were coherent as compared to all these data and located on a curve of similar shape to that obtained by Dyban with the same turbulence intensity. There was, however, systematically a difference of about 20% between these two curves. This discrepancy could be explained by the difference in the temperature profile at the cylinder surface. The constant heat flux method generates great differences between the surface temperatures while these temperatures are nearly the same using the psychrometric method.

In order to evaluate the systematic errors, $E_{1h}$ and $E_{1k}$, depending on the calculation method, formulas (24) and (25) were digitised on 13 points. The temperatures were calculated from polynomial interpolations on the measured five temperatures. Dyban's results were used to determine the local transfer coefficients by using a function $f$. Since $h/k$ and $\bar{h}/\bar{k}$ were identical according to (15) it was possible to define $f$ equal to $h/\bar{h}$ or $k/\bar{k}$.

The $f$ function can be calculated from the work of Dyban *et al.* [19] for two turbulence intensities 0.3 and 12%. For $Tu = 0.3\%$, $f$ varied slightly according to the Reynolds number while it can be considered as unique for $Tu = 12\%$. In the present experimental

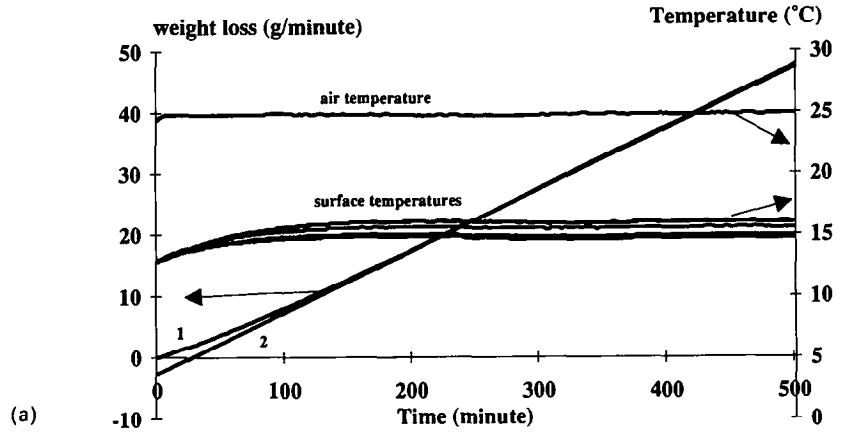


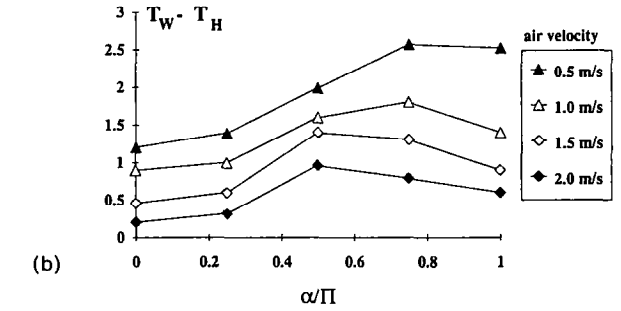


FIG. 3. (a) Air temperature, evolution of the surface temperatures and weight loss during an experiment. (1) Experimental weight loss, (2) regression based on the weight loss during the steady-state period; (b) Differences between temperatures on the circular cylinder ($\phi = 0.1$ m) surface and wet bulb temperature for four air velocities ($\alpha/\pi$ is the dimensionless angular coordinate).

field ($Tu = 12\%$, $3500 < Re < 26\,000$), it is thus possible to simplify equations (24) and (25) in:

$$E_{1h} = \frac{1}{13(T_\infty - \bar{T}_w)} \sum_{13} \left( f(T_w - \bar{T}_w) + \frac{\varepsilon\sigma(T_w^4 - (\bar{T}_w)^4)}{\bar{h}} \right) \quad (32)$$

$$E_{1k} = \frac{1}{13(P(T_{dew}) - P(\bar{T}_w))} \sum_{13} f(P(T_w) - P(\bar{T}_w)). \quad (33)$$

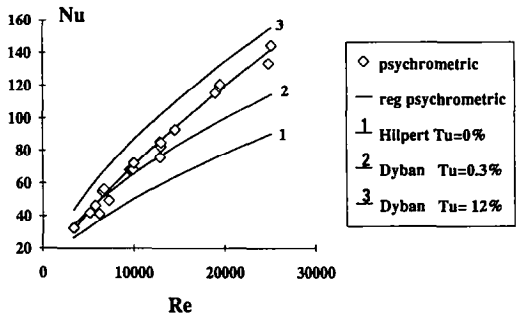


FIG. 4. Comparison of mean Nusselt numbers determined by the psychrometric method at $Tu = 12\%$ with results of Hilpert ($Tu = 0\%$) and Dyban ($Tu = 0.3\%$ and 12%).

The methodological relative errors on $\bar{h}$ and on $\bar{k}$, calculated from the 24 experiments were: $E_{1h} = -1.8\% \pm 0.5\%$ and $E_{1k} = +2.4\% \pm 0.6\%$. $E_{1h}$ is a systematic error by default and $E_{1k}$ by excess. Within the experimental range, their amplitudes were comparable and did not depend on air velocity.

The relative errors on $\bar{h}$ and $\bar{k}$ related to the measurement, $E_{2h}$ and $E_{2k}$, were calculated assuming independent errors on $T_\infty$ and $T_w$: $\Delta(T_\infty) = \pm 0.1°C$, $\Delta(T_w) = \pm 0.1°C$, $\Delta(T_{dew}) = \pm 0.1°C$. For all experiments, we get: $E_{2h} = \pm 1.7\%$, $E_{2k} = \pm 2.0\%$. These errors varied little with air velocity.

With the aim of testing the improvement of accuracy resulting from a rise in air temperature, $T_\infty$, $E_{2h}$ and $E_{2k}$ were calculated for the following conditions: dew point temperature of 2.0°C and $T_\infty$ ranging between 10 to 40°C. This corresponded to a good compromise between a high accuracy and a sufficiently long steady-state period. The body surface temperatures were recalculated from equations (17) using the experimental values of $h$ and $k$ and the previously defined $f$ function for a turbulence intensity of 12%. Figure 5 shows that $E_{2h}$ and $E_{2k}$ decreased exponentially from about 3.5 to about 1.0% for $T_\infty$ ranging between 15 and 40°C. For $T_\infty = 25°C$, we get: $E_{2h} = \pm 1.5\%$ and $E_{2k} = \pm 2.0\%$ which corresponds to the values calculated previously from the

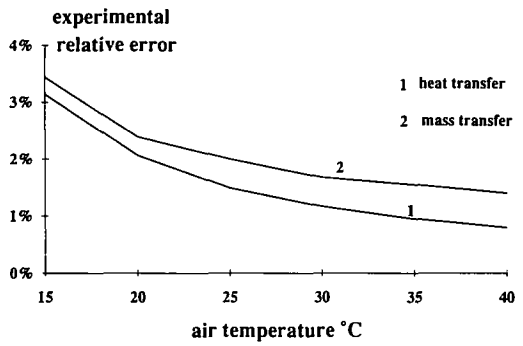


FIG. 5. Variation in the relative error of mean transfer coefficient with air temperature.

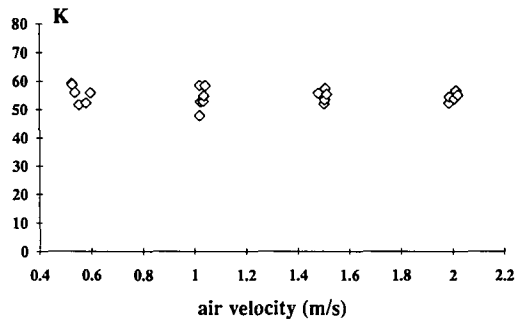


FIG. 6. Ratio of heat to mass transfer coefficients ($K$) calculated from the experimental results at different air velocities.

experimental data. Other calculations have shown that beyond an air temperature of 40°C, $E_{2h}$ goes on decreasing with $T_\infty$ while $E_{2k}$ gets stabilised. This supports the idea developed in the theoretical part that the accuracy of $\bar{h}$ increases continually with $T_\infty$ while there is an optimum temperature for the determination of $\bar{k}$ (around 40°C). If the measurements of surface temperature and air temperature are experimentally dependent, the errors become lower than 0.5% as soon as $T_\infty$ becomes higher than 15°C. This leads to the possibility of improving the accuracy of the method in future experiments. Using an infra-red camera it will be possible to measure both: $T_\infty$ on a piece of dry plaster in air, and the surface temperatures of the wetted body, $T_w$. If the emissivities of dry and wet plaster are similar, $T_\infty$ and $T_w$ will be dependent and the experimental error can be considered as minor. Only the methodological error with a value of about 2% will remain.

For air velocities over 2.0 m s$^{-1}$, the psychrometric method is reliable for measuring mean transfer coefficients. The only theoretical limit consists in not considering the heat exchanges by compression and by friction, but rather the heat exchanges by convection. However, from a practical point of view, increasing the air velocity decreases the steady-state period. Hence, there is an air velocity limit according to experiments beyond which the psychrometric method cannot be used. This air velocity limit depends on the other experimental conditions, i.e. air temperature and wetted body dimensions.

*Ratio of heat transfer coefficient to mass transfer coefficient*

All experimental values concerning the ratio of heat to mass transfer coefficient, $K$, are given in Fig. 6. The dispersion of results is larger for low air velocities probably because of a larger error on the determination of mean surface temperature for velocities lower than 1 m s$^{-1}$. The mean of $K_{exp}$ for the 24 experiments is: $54.8 \pm 0.6$. This value might be corrected on account of the systematic methodological error by default on $\bar{h}$ ($E_{1h} = -1.8\%$) and by excess on $\bar{k}$ ($E_{1k} = +2.4\%$), it then follows: $K_{exp} = 57.0 \pm 0.6$.

Table 4 indicates the values of the $K_{th}$ ratio for three values of $n$ (0.4, 0.5, 0.66), for temperatures ranging between 0 and 25°C and for two different atmospheric pressures, 101 323 and 91 990 Pa. The second value corresponds to the atmospheric pressure due to the altitude at the site of the experiment. The values of $K_{th}$ are not very different from each other with $n = 0.4$, 0.5 or 0.66. In addition, for temperatures ranging from 13 to 15°C, which correspond to the surface temperatures of the plaster during the experiments, the $K_{th}$ values are close, apart from the measurement errors, to the corrected experimental value.

*Determination of local transfer coefficients*

As in the case of mean transfer coefficients, it is possible to determine the influence that the variation of air temperature between 10 and 40°C would exert on the accuracy of determination of the local coefficients. The errors which only depend on $T_\infty$ and on the local value of the body surface temperature $T_w$, were evaluated for four air velocities (0.5, 1.0, 1.5, 2.0 m s$^{-1}$) and for two surface positions on the circular cylinder, i.e. points where $T_w$ was minimum, Fig. 7(a), and maximum, Fig. 7(b). In any case, the accuracy increases when the convective exchanges decrease relative to the radiative exchanges. This is either because the temperature of the air rises or because its velocity falls, or for constant air temperatures and velocities, when the boundary layer becomes thicker over the body surface. This always results in the fact that the accuracy at the body surface increases with increasing $T_w$. In all cases, using $K_{exp}$ instead of $K_{th}$ minimises the experimental errors by about 2%. Furthermore, comparison of Fig. 7(a) and (b) shows that these errors can be divided by 2 or 3 if the same probe is used to measure both the air and the surface temperatures. In the present experiment, the temperature probes were different and the air temperature was 25°C. The calculated error then oscillated between $\pm 7\%$ in the most favourable case ($T_w$ maximum, $U_\infty = 0.5$ m s$^{-1}$) and $\pm 20\%$ in the most unfavourable case ($T_w$ minimum, $U_\infty = 2.0$ m s$^{-1}$) which seems to render the method infeasible. These errors seem large, as in fact they are, but one must keep in mind that

Table 4. Theoretical values of heat to mass transfer ratio $K_{th}$ (equation 15)

| | $P_{atm}$ = 101 323 Pa | | | $P_{atm}$ = 91 990 Pa | | |
|---|---|---|---|---|---|---|
| $T_w$°C | $n$ = 0.4 | $n$ = 0.5 | $n$ = 0.666 | $n$ = 0.4 | $n$ = 0.5 | $n$ = 0.666 |
| 0 | 61.6 | 60.5 | 58.9 | 55.9 | 55.0 | 53.5 |
| 5 | 61.9 | 60.9 | 59.3 | 56.2 | 55.3 | 53.8 |
| 10 | 62.3 | 61.3 | 59.7 | 56.5 | 55.6 | 54.2 |
| 15 | 62.7 | 61.7 | 60.1 | 56.9 | 56.0 | 54.6 |
| 20 | 63.1 | 62.2 | 60.6 | 57.3 | 56.4 | 55.0 |
| 25 | 63.6 | 62.6 | 61.1 | 57.7 | 56.9 | 55.5 |

these are estimates of the maximum possible error of the method. In practice one can expect to do better than this.

For a turbulence intensity of 12%, the results obtained in this study and put in the form of an $f$ function are compared to those of Dyban in Fig. 8. The curves obtained with the psychrometric method for air velocities from 1.0 to 2.0 m s$^{-1}$ are in good agreement with the experimental curve of Dyban. Moreover, there is only a maximum difference of 10% between the experimental findings, indicating that the former calculation error was pessimistic. For an air velocity of 0.5 m s$^{-1}$, there is an overlapping of the results of the two trials, but they are separated from Dyban's curve. Further investigation is needed to explain this difference.

In the present experimental conditions, the psychrometric method was less accurate for determining local transfer coefficients than for determining mean transfer coefficients. However, as in the case of mean coefficients, it would be possible to improve considerably the accuracy of determination of local coefficients by performing the experiment at an air temperature of 40°C and by using the same temperature probe to measure both air and surface temperatures. The errors would then be less than 3% for air velocities between 0 and 2.0 m s$^{-1}$. For air velocities higher than 2.0 m s$^{-1}$, the ratio between the amount of heat exchanged by radiation and that exchanged by convection decreases. Accordingly, the errors on the determination of local transfer coefficients are so great that the psychrometric method cannot be used. It would be possible to cope with this problem by adding infra-red radiation to the experimental device. However, the determination of local transfer coefficients by a simple psychrometric method should most likely be confined to low air velocities.

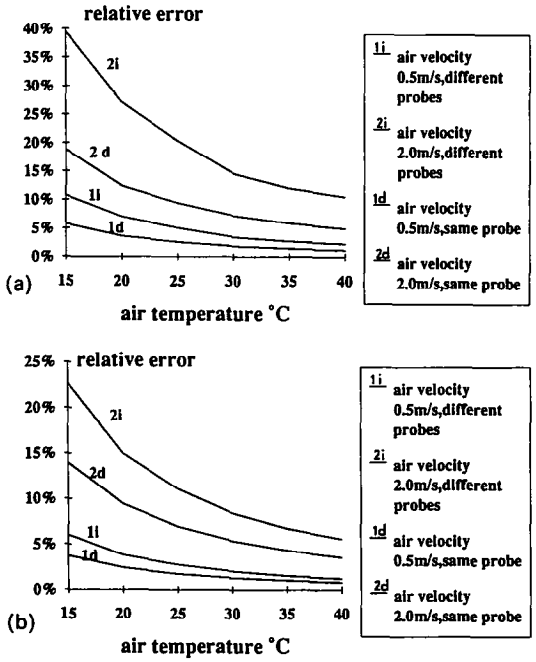


FIG. 7. Variation in the relative error of local transfer coefficients: (a) at the stagnation point for two air velocities with air temperature; (b) at the point where $T_w$ is maximum (close to the separation point) for two air velocities with air temperature.

## 5. CONCLUSION

This study shows that in the present experimental conditions, the psychrometric method allows easy and accurate measurements of heat and mass mean transfer coefficients. In addition, assuming the nonvariance of the ratio $h/k$ during a simultaneous heat and mass transfer at any point of the body surface, a simple temperature measurement at any point of that surface makes possible the determination of local transfer

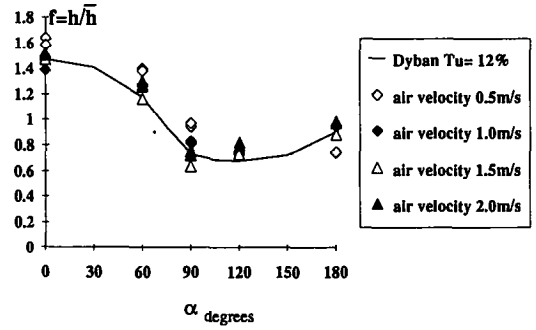


FIG. 8. Comparison of the variation of the local heat transfer coefficient around a circular cylinder determined by the psychrometric method, in form of $f$ function, with Dyban's results at $Tu$ = 12%.

coefficients whatever the complexity of the body. However, the accuracy of this determination should be further improved.

These two possibilities render the utilisation of the psychrometric method very flexible. Thus, in the context of applied studies, the mean coefficients of heat and mass transfers around a large number of bodies of different shapes and dimensions can be readily and rapidly determined by measuring weight losses and some surface temperatures. In contrast, for fine analysis of heat and mass transfers around a body of a complex shape, the two possibilities should be used conjointly. The determination of mean transfer coefficients would enable one to check both the running of the experiment and the constancy of the ratio between heat and mass coefficients. This hypothesis is the cornerstone of the determination of local transfer coefficients by the psychrometric method. While this is not of major importance for the food industry, the determination of local transfer coefficients by a simple psychrometric method is restricted to air velocities lower than 2.0 m $s^{-1}$.

*Acknowledgements*—The authors wish to thank Professor M. Martin (INPL (LEMTA) 540501 Nancy, France) for his advice and K. Rérat (INRA-CRJJ, Unité Centrale de Documentation, 78352 Jouy-en-Josas Cedex, France) for the translation into English.

## REFERENCES

1. N. M. Ozisik, *Heat Transfer a Basic Approach*, pp. 368, 381, 725. McGraw-Hill, New York (1985).
2. Y. Katto, H. Koizumi and T. Yamaguchi, Turbulent heat transfer of a gas flow on an evaporation liquid surface, *Bull. J.S.M.E.* **18**, 866–873 (1975).
3. J. Kestin and R. T. Wood, The influence of turbulence on mass transfer from cylinders, *J. Heat Transfer* **93**, 321–327 (1971).
4. J. S. Lewis, Heat transfer predictions from mass transfer measurements around a single cylinder in cross-flow, *Int. J. Heat Mass Transfer* **14**, 325–329 (1971).
5. R. J. Dahlen, A relation between heat and mass transfer coefficients verified for adiabatic evaporation from a cylinder, Ph.D. Thesis, Purdue University (1962).
6. M. Martin and M. Lebouché, A propos de l'analogie entre transfert de chaleur et transfert de masse en régime de couche limite. Application au cas du cylindre frontal en régime de convection forcée, Réunion d'études du groupement universitaire de thermique 13 Nov 1975.
7. K. Torii, M. Isobe, N. Miura and T. Horikoshi, Free stream turbulence effect on heat transfer from spheres, *Bull. J.S.M.E.* **24**, 131–137 (1981).
8. T. K. Sherwood, The drying of solids—I, *Ind. Engng Chem.* **21**, 12–16 (1929).
9. J. G. Brennan, J. R. Butters, N. D. Cowell and A. E. V. Lilly, *Food Engineering Operations*, p. 532. Applied Science Publishers, London (1976).
10. C. J. Geankoplis, *Transport Processes and Unit Operations*, p. 862. Allyn and Bacon, Boston (1983).
11. J. J. Bimbenet, 4ème cahier du G.I.A, p. 13, *SEPAIC* (1978).
12. M. Loncin and R. L. Merson, *Food Engineering and Selected Applications*, p. 494. Academic Press, New York (1979).
13. I. L. Ryhming, *Dynamique des Fluides*, p. 101. Presse polytechnique Romande (1984).
14. J. E. Maneval, M. J. McCarthy and S. Whitaker, Studies of the drying process by NMR imaging. In *Drying* **91**, 170–180. Elsevier Science Publishers, Amsterdam (1991).
15. J. D. Daudin and M. L. V. Swain, Heat and mass transfer in chilling and storage of meat, *J. Food Engng* **12**, 95–116 (1990).
16. A. Fornell, Séchage des produits biologiques par l'air chaud—calcul des séchoirs, Thèse de Docteur Ingénieur E.N.S.I.A. (1979).
17. A. Kondjoyan, Détermination des coéfficients de transfert par psychrométrie, D.E.A Université B. Pascal, Clermont-Fd (1989).
18. N. N. Mohsenin, *Thermal Properties of Foods and Agricultural Materials*, p. 296. Gordon and Breach, New York (1980).
19. E. P. Dyban, E. Ya. Epick and L. G. Kozlova, Combined influence of turbulence intensity and longitudinal scale and air flow acceleration on heat transfer of circular cylinder, *5th Heat Transfer Conf.*, F.C.8.4, pp.310–314. Tokyo (1974).
20. W. H. MacAdam, *Heat Transmission* (3rd Edn), p. 258. McGraw-Hill, New York (1954).
21. V. T. Morgan, The overall convective heat transfer from smooth circular cylinders, *Adv. Heat Transfer* **11**, 199–264 (1975).
22. T. Ota, H. Nishiyama and Y. Taoka, Heat transfer and flow around an elliptic cylinder, *Int. J. Heat Mass Transfer* **27**, 1771–1779 (1984).

## APPENDIX

*Measurements errors on mean transfer coefficients*

Differentiating equations (22) and (23), if $\Delta(\phi_m)$, $\Delta(T_\infty)$ and $\Delta(T_w)$ are assumed to be independent we get:

$$E_{2h} = \left|\frac{L_{vap}}{A}\right| \Delta(\bar{\phi}_m) + \left|\frac{4\varepsilon\sigma T_\infty^3}{A} - \frac{1}{B}\right| \Delta(T_\infty) + \left|\frac{1}{B} - \frac{4\varepsilon\sigma \bar{T}_w^3}{A}\right| \Delta(\bar{T}_w)$$

$$E_{2k} = \left|\frac{\Delta(\bar{\phi}_m)}{\bar{\phi}_m}\right| + \left|\frac{dP(\bar{T}_w)/d\bar{T}_w}{P(\bar{T}_w) - P(T_{dew})}\right| \Delta(\bar{T}_w) + \left|\frac{dP(T_{dew})/dT_{dew}}{P(\bar{T}_w) - P(T_{dew})}\right| \Delta(T_{dew})$$

with:

$$A = \bar{\phi}_m L_{vap} + \varepsilon\sigma(T_\infty^4 - (\bar{T}_w)^4) \quad B = (T_\infty - \bar{T}_w).$$

If the air and surface temperatures are measured with the same probe and with an error of $\Delta T$, $E_{2h}$ can be simplified:

$$E_{2h} = \left|\frac{L_{vap}}{A}\right| \Delta(\bar{\phi}_m) + \left|\frac{4\varepsilon\sigma(T_\infty^3 - (\bar{T}_w)^3)}{B}\right| \Delta(T)$$

*Measurement errors on local transfer coefficients*

The $H1$, $H2$, $H3$ functions obtained by differentiation of equation (27) are:

In the case where $K_{th}$ is used and $E = (T_w - T_\infty) + (P(T_w) - P(T_{dew}))/K$:

$$H1 = \frac{4T_\infty^3}{(T_\infty^4 - T_w^4)} + \frac{1}{E}$$

$$H2 = \frac{-4T_w^3}{(T_\infty^4 - T_w^4)} - \frac{1 + (dP(T_w)/dT_w)/K_{th}}{E}$$

$$H3 = \frac{(dP(T_{dew})/dT_{dew})}{K_{th}E}$$

and in the case where the constant $K$ is calculated by means of the mean coefficients determined for the same experiment :

$$H1 = \frac{4T_{\infty}^3}{(T_{\infty}^4 - T_w^4)}\left(1 + \frac{P(T_w) - P(T_{dew})}{EK_{exp}}\right) - \frac{P(T_w) - P(T_{dew})}{EK_{exp}(T_{\infty} - \bar{T}_w)} + \frac{1}{E}$$

$$H2 = \frac{-4T_w^3}{(T_{\infty}^4 - T_w^4)} - \frac{4\bar{T}_w^3[P(T_w) - P(T_{dew})]}{(T_{\infty}^4 - \bar{T}_w^4)EK_{exp}} + \frac{(dP(\bar{T}_w)/d\bar{T}_w)}{EK_{exp}} - \frac{(dP(T_w)/dT_w)}{EK_{exp}} - \frac{1}{E}$$

$$H3 = \frac{(dP(T_{dew})/dT_{dew})}{K_{exp}E}\left(1 - \frac{P(T_w) - P(T_{dew})}{P(\bar{T}_w) - P(T_{dew})}\right).$$